Preparation and Characterization of α-D-Glucopyranosyl-α-acarviosinyl-D-glucopyranose, a Novel Inhibitor Specific for Maltose-Producing Amylase†

Myo-Jeong Kim,‡ Hee-Seob Lee,‡ Jin-Sook Cho,‡ Tae-Jip Kim,§ Tae-Wha Moon,‡ Sang-Taek Oh,|| Jung-Wan Kim,⊥ Byung-Ha Oh,|| and Kwan-Hwa Park*,‡

Research Center for New Bio-Materials in Agriculture and Department of Food Science & Technology, School of Agricultural Biotechnology, Seoul National University, Suwon 441-744, Korea, Department of Food Science and Technology, Chungbuk National University, Cheongju 361-763, Korea, Department of Life Science, Division of Molecular and Life Science, Pohang University of Science and Technology, Pohang 790-784, Korea, and Department of Biology, University of Incheon, Incheon 402-749, Korea

Received January 24, 2002; Revised Manuscript Received April 29, 2002

ABSTRACT: A novel inhibitor against maltose-producing α-amylase was prepared via stepwise degradation of a high-molecular-weight acarbose (HMWA) using *Thermus* maltogenic amylase (ThMA). The structure of the purified inhibitor was determined to be α-D-glucopyranosyl-α-acarviosinyl-D-glucopyranose (GlcAcvGlc) by ^{13}C NMR and MALDI-TOF/MS. Progress curves of PNPG2 hydrolysis by various amylolytic enzymes, including MGase, ThMA, and CDase I-5, in the presence of acarbose or GlcAcvGlc indicated a slow-binding mode of inhibition. Analytical ultracentrifugation and X-ray crystallography analyses revealed that the presence of GlcAcvGlc increased the dimerization of ThMA. The formation of dimer complexed with GlcAcvGlc might induce a conformational change in ThMA, leading to a two-step inhibition process. The inhibition potency of GlcAcvGlc for MGase, ThMA, and CDase I-5 was 3 orders of magnitude higher than that of acarbose.

Acarbose is widely recognized as a potent inhibitor of several carbohydrases, including α-glucosidase (*1*), glucoamylase (*2*, *3*), α-amylase (*1*, *4*, *5*), and cyclomaltodextrin glucanotransferase (CGTase[1]; *6*, *7*). Acarbose is a pseudotetrasaccharide in which acarviosine, a pseudo sugar ring (4,5,6-trihydroxy-3-[hydroxymethyl]-2-cyclohexen-1-yl) linked to the nitrogen of 4-amino-4,6-dideoxy-D-glucopyranose (4-amino-4-deoxy-D-quinovopyranose), is linked to maltose by a α-(1→4)-glycosidic bond (Figure 1A). Acarbose, an inhibitor most potent against α-glucosidase, is produced by *Actinoplanes* sp. This species also produces a high-molecular-weight acarbose (HMWA), which is an excellent inhibitor of α-amylase (*1*). HMWA is a mixture of homologue series with 7−30 glucose units linked to acarviosine. Since the only difference between HMWA and acarbose is the number of glucose units attached to acarviosine, the length of glucose chain determines the specificity of a target enzyme.

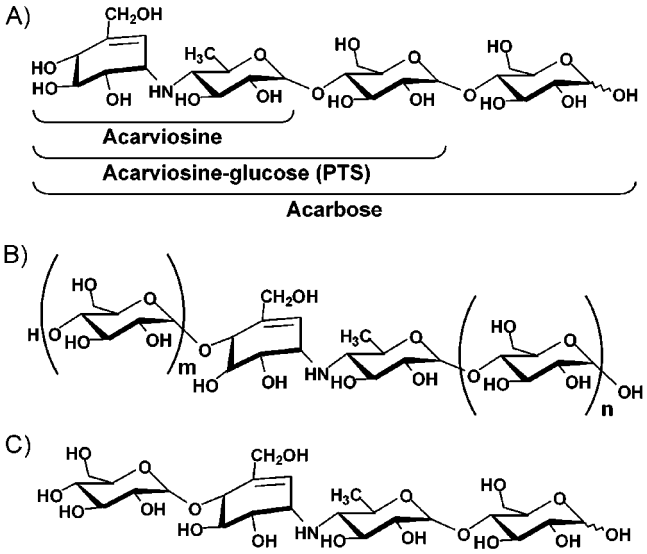

FIGURE 1: Structures of the amino sugars having inhibitory effects on amylase activity. A, acarbose; B, high-molecular-weight acarbose (HMWA); and C, α-D-glucopyranosyl-α-acarviosinyl-D-glucopyranose.

† This work was supported by a grant for the G7 project from Korean Science and Engineering Foundation and Technology and in part by the Brain Korea 21 Project from the Korean Ministry of Education and the NRL program (2001) from the Korean Ministry of Science.

* To whom correspondence should be addressed. Telephone: +82-31-290-2582. Fax: +82-31-294-1336. E-mail: parkkh@plaza.snu.ac.kr.

‡ Seoul National University.

§ Chungbuk National University.

|| Pohang University of Science and Technology.

⊥ University of Incheon.

[1] Abbreviations: BBMA, *Bacillus subtilis* maltogenic amylase; BLMA, *Bacillus licheniformis* maltogenic amylase; BSMA, *Bacillus stearothermophilus* maltogenic amylase; CDase I-5, cyclomaltodextrinase from alkalophilic *Bacillus* sp. I-5; CGTase, cyclomaltodextrin glucanotransferase; α-CHCA, α-cyano-4-hydroxycinnamic acid; DNS, dinitrosalicylate; G2-acarbose, maltosyl-acarbose; GlcAcvGlc, α-D-glucopyranosyl-α-acarviosinyl-D-glucopyranose; HMWA, high-molecular-weight acarbose; HMBC, heteronuclear multiple bond connectivity; HPIC, high performance ion chromatography; MALDI-TOF, matrix-assisted laser desorption ionization time-of-flight; MGase, maltogenase; NMR, nuclear magnetic resonance; PNPG2, *p*-nitrophenyl-α-D-maltoside; PPA, porcine pancreatic α-amylase; ThMA, *Thermus* maltogenic amylase; TLC, thin-layer chromatography; PTS, pseudotrisaccharide or acarviosine-glucose.

10.1021/bi025586b CCC: $22.00
Published on Web 06/27/2002

Scheme 1

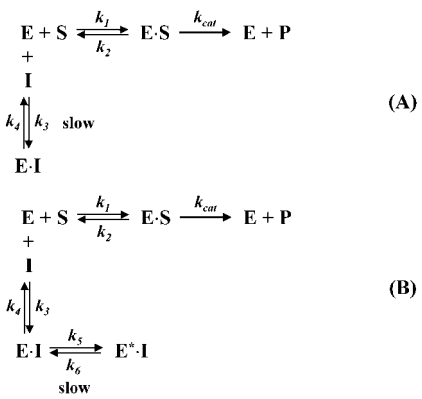

Activity assays in the presence of inhibitors such as acarbose and methyl acarviosinide on a wild type and a mutant glucoamylase showed that the K_i values of the enzymes varied depending on the structure of each inhibitor (*8*). Park et al. (*9*) produced various acarbose derivatives using the transglycosylation reaction of maltogenic amylases from *Bacillus stearothermophilus* (BSMA) and *Thermus* (ThMA). Among the derivatives produced, isoacarbose was found to be a potent inhibitor for porcine pancreatic α-amylase (PPA) (*7*). Development of acarbose derivatives as amylolytic enzyme inhibitors provides a new approach for the management of diabetes (*10*, *11*). And it also provides a useful tool for screening a novel inhibitor against a target enzyme (*7*).

Slow binding, or time-dependent inhibition, is a widespread phenomenon among potent glycosidase inhibitors (*12*−*15*), where the inhibition process is relatively slow, occurring over a period of minutes or longer. Further studies on slow inhibition are required to get more detailed insight into the binding mode of potent glycosidase inhibitors. From the kinetic point of view, most reversible time-dependent inhibition is related with one of the two mechanisms depicted in Scheme 1 (*16*).

In mechanism A, the inhibitor binds to the enzyme in a simple bimolecular reaction in a single step, but the association and dissociation rate constants (k_3 and k_4, respectively) are such that equilibrium is established slowly. In mechanism B, binding between the enzyme and the inhibitor may have an initial fast-binding step establishing equilibrium that is defined by the on and off rate constants k_3 and k_4, just as in mechanism A. However, binding of the inhibitor induces a reversible conformational transition or isomerization of the enzyme, leading to a tightly bound enzyme−inhibitor complex E*•I, where the forward and reverse rate constants for the equilibrium between these two inhibitor-bound conformations of the enzyme are given by k_5 and k_6, respectively.

In this study, a hydrolysis product of HMWA was obtained by the action of ThMA, and its structure and physicochemical properties were characterized. In addition, the efficacy and specificity of the inhibitor, α-D-glucopyranosyl-α-acarviosinyl-D-glucopyranose (GlcAcvGlc), on maltose-producing enzymes such as maltogenase, maltogenic amylase, and cyclomaltodextrinase were also investigated.

MATERIALS AND METHODS

Microorganisms, Enzymes, and Reagents. Actinoplanes sp. KCTC9162 was cultured in YMG medium (1.0% malt extract, 0.3% glucose, and 0.3% yeast extract) at 28 °C. *Escherichia coli* MC1061 [F⁻, *araD*139, *recA*13, Δ(*araABC-leu*)7696, *galU*, *galK*, Δ*lacX*74, *rpsL*, *thi*, *hsdR*2, *mcrB*] harboring a plasmid containing the ThMA gene was cultured in a Luria-Bertani (LB) medium (1% Bactotryptone, 0.5% yeast extract, and 0.5% NaCl) supplemented with ampicillin (100 μg/mL) at 37 °C.

Maltogenase (MGase) 4000L was kindly provided by Novo Nordisk (Bagsvaerd, Denmark). ThMA was purified from the recombinant *E. coli* strain as described previously (*17*). Cyclomaltodextrinase of alkalophilic *Bacillus* sp. I-5 (CDase I-5) was purified from the *E. coli* strain carrying the corresponding gene as described previously (*18*). Maltase and sucrase from rat intestine were kindly donated by Dr. Hye-Young Kim at Korea Food Research Institute (Sungnam, Korea). Porcine pancreatic α-amylase and sweet potato β-amylase were purchased from Sigma (St. Louis, MO). Pure acarbose (96%, w/w) was provided generously by Bayer Korea (Seoul, Korea). *p*-Nitrophenyl-α-D-maltoside (PNPG2) was purchased from Calbiochem (San Diego, CA). All other reagents used for inhibition kinetics were reagent-grade.

Preparation of GlcAcvGlc from HMWA. For the production of HMWA, *Actinoplanes* sp. KCTC9162 was cultured in starch medium (5% soluble starch, 1% yeast extract, 0.2% K_2HPO_4). Two hundred milliliters of fresh medium containing 6 g of glass beads was prepared in a 500 mL baffled bottom flask and autoclaved at 121 °C for 15 min. *Actinoplanes* sp. KCTC9162 was inoculated into the sterilized medium and cultured at 28 °C for 3−5 days in a shaking incubator (300 rpm, 8480-SF, Vision Science Co., Buchon, Korea). The pH of the culture broth was adjusted to 2.5 with 0.1 M of HCl and stirred at ambient temperature for 2 h after activated charcoal (30 g/L; Sigma) was added. The mycelium and charcoal was discarded by centrifugation at 8000 g for 15 min (VS-15, Vision Science Co.). The pH of the supernatant was readjusted to 6 with 0.1 M NaOH and concentrated by 10 folds using a rotary vacuum evaporator (EYELA, Tokyo, Japan). Starch and long-chain dextrins in the concentrated supernatant (20 mL) were precipitated by adding 80 mL of methanol. After removal of sediment by centrifugation (4000 g, 5 min), 800 mL of ethanol was added to 100 mL of the supernatant. Finally, HMWA was collected by centrifugation and dissolved in 200 mL of 50 mM sodium acetate buffer (pH 6.0).

To produce GlcAcvGlc, we incubated HMWA solution (200 mL) with 25 400 U of ThMA (127 U/mL) at 55 °C for 24 h. HMWA hydrolysate was filtrated using an ultrafiltration kit (150 mL capacity, Millipore, Bedford, MA) with YM10 membrane (MW cutoff = 10000, Millipore). The filtrate was concentrated using a SpeedVac (Savant, Holbrook, NY), and the concentrate was loaded onto a BioGel P-4 column (1.5 × 100 cm, 45−90 μm bead size, BioRad, Hercules, CA). The fractions with inhibition activity against ThMA were concentrated and loaded onto a BioGel P-2 column (1.5 × 100 cm, 45−90 μm bead size, BioRad). Then the major fractions were applied to a CM-cellulose column (3 × 12 cm, 25−60 μm bead size, Sigma) that was pre-equilibrated with distilled water and desorbed with 0.1M NaCl. The GlcAcvGlc fractions were collected and concentrated using a SpeedVac. Finally, the concentrated sample was desalted using a BioGel P-2 column (1.5 × 100 cm). The GlcAcvGlc

fractions were collected and lyophilized for future uses. About 50 mg of GlcAcvGlc was obtained from a liter of culture supernatant.

Enzyme Assay. ThMA activity was assayed at 55 °C by the dinitrosalicylate (DNS) method using 0.5% (w/v) cyclomaltoheptaose dissolved in 50 mM sodium acetate buffer (pH 6.0) as a substrate (*17*). One unit (U) of the enzyme activity was defined as the amount of enzyme that split 1 μmol equivalent of glycosidic bond in the substrate in one minute under the reaction conditions.

Progress Curve Determinations. All reactions were carried out using PNPG2 as a substrate in 50 mM sodium phosphate buffer (pH 7.0) at 40 °C. Enzyme activities were measured continuously using Ultrospec III spectrophotometer (Pharmacia, Uppsala, Sweden). Two hundred and fifty microliters of 20 mM PNPG2 and 50 μL of inhibitor at various concentrations were transferred into a cuvette (1 cm pathlength, 1 mL capacity), which was preheated for 5 min in a water-jacketed turret circulated with 40 °C water. Enzyme solution prewarmed at 40 °C for 5 min (200 μL) was added to the preheated substrate−inhibitor mixture. The total elapsed time between enzyme addition and the initiation of data collection was less than 15 s. The formation of *p*-nitrophenol was monitored continuously at 400 nm. The data were analyzed using the nonlinear regression program of SigmaPlot (SPSS Inc., Chicago, IL) to give the individual parameters for each progress curve: v_0 (initial velocity), v_s (steady-state velocity), and k_{obs} (apparent first-order rate constant for the transition from v_0 to v_s) according to eq 1 (*16*):

$$[P] = v_s t + (v_0 - v_s)[1 - \exp(-k_{obs} t)]/k_{obs} \qquad (1)$$

where P is the *p*-nitrophenol formed and represented by the A_{400nm} increase and t is the reaction time. K_m values of PNPG2 for each enzyme were determined from Lineweaver−Burk plot (*19*).

Determination of IC_{50}. The IC_{50} of an inhibitor was determined as the concentration of the inhibitor causing decrease of an enzyme activity by 50%. The enzyme activity was measured using the glucose oxidase−peroxidase method (*20*) for maltase and sucrase or the DNS method (*17*) for α-amylase, β-amylase, and ThMA. Following a 10 min preincubation of an enzyme with various concentrations of an inhibitor, the reaction was initiated by adding the enzyme−inhibitor mixture to an appropriate substrate solution (maltose for maltase; sucrose, sucrase; soluble starch, α- and β-amylase; and cyclomaltoheptaose, ThMA). The reaction was maintained for 10 min at 37 °C (55 °C for ThMA).

Thin-Layer Chromatography (TLC) and High-Performance Ion Chromatography (HPIC) Analyses. The reaction mixtures were analyzed by TLC using Whatman K6F silica gel plates (Fischer Scientific, Pittsburgh, PA) and a solvent system of ethyl acetate/isopropyl alcohol/water (1:3:1, v/v/v). After being developed twice, the TLC plate was dried and visualized by dipping into a solution containing 0.3% (w/v) *N*-(1-naphthyl)-ethylenediamine and 5% (v/v) H_2SO_4 in methanol and heated at 110 °C for 10 min. For HPIC analysis, the reaction mixture was diluted with water and filtered using a membrane filter kit (0.45 μm pore diameter, Pall Life Sciences, Ann Arbor, MI). Twenty microliters of the sample was applied to a Carbopak PA1 column (0.4 × 25 cm, Dionex, Sunnyvale, CA) and eluted with a 0−30% of 600 mM sodium acetate gradient in 150 mM NaOH at a flow rate of 1.0 mL/min.

Nuclear Magnetic Resonance (NMR) Analysis. The ^{13}C NMR spectrum was recorded using a JNM LA-400 FT-NMR spectrometer (JEOL, Tokyo, Japan) and Heteronuclear Multiple Bond Connectivity (HMBC) mode.

Matrix-Assisted Laser Desorption Ionization Time-of-Flight (MALDI-TOF) Mass Spectrometer Analysis. The MALDI-TOF mass spectrum was collected using a Voyager-DE (Perseptive Biosystem, Framingham, MA) system. As a matrix, α-cyano-4-hydroxycinnamic acid (α-CHCA, Sigma) was used. One microliter of the purified sample and α-CHCA was dropped on a sample applicator and dried well. Then, the sample plate was placed in the Voyager-DE Biospectrometry workstation operated with acceleration voltage of 20 kV.

Analytical Ultracentrifugation. Sedimentation equilibrium measurements were performed using a Beckman Optima XL-A analytical ultracentrifuge (Beckman Coulter, Inc., Fullerton, CA) equipped with a four-hole rotor with standard either two or six channel cells at a rotor speed of 10,000 rpm. The absorbance-versus-radius distributions $A(r)$ were recorded at 280 nm, and the dissociation constant (K_d) was calculated according to Kim et al. (*21*).

Crystallography. ThMA crystals were obtained by vapor diffusion from droplets of 2 μL of protein (10 mg/mL in 20 mM maleate, pH 6.8) and 0.5 μL of a precipitant solution containing 0.5 M lithium sulfate, 0.3 M ammonium sulfate, and 0.1 M sodium citrate (pH 5.6) in 4% ethanol (v/v), which were equilibrated against 1 mL of the same precipitant solution at 22 °C (*22*). The crystals of ThMA in complex with GlcAcvGlc were obtained by soaking the native crystal with 1 mM of an inhibitor. Diffraction data to 2.55 Å were obtained from a flash-cooled crystal using the synchrotron X-ray beamline BL6B at Photon Factory (Tsukuba, Japan). The details of X-ray data collection, structure determination, and refinement were described previously (*22*).

RESULTS

Production of GlcAcvGlc. Actinoplanes sp. KCTC9162 produced acarbose in the culture broth when maltose or glycerol was added as a carbon source (*1*). On the other hand, HMWA, much longer compounds with strong inhibition activity against α-amylase, were produced in the presence of starch. They have an acarviosine core structure in which 7−30 of D-glucose units are linked at both sides (Figure 1B). To produce large amounts of HMWA, we cultured *Actinoplanes* sp. KCTC9162 for 7 days in starch medium. The culture broth turned dark to black as the growth proceeded. Strong inhibition activity against α-amylase was found in the cell-free supernatant.

HMWA was hydrolyzed with ThMA for the production of GlcAcvGlc (Figure 2). ThMA degraded HMWA readily to maltose and smaller compounds, including GlcAcvGlc. GlcAcvGlc was not further hydrolyzed by ThMA and accumulated in a considerable amount. Since GlcAcvGlc itself is an inhibitor for maltogenic amylases (discussed below), the hydrolysis rate of HMWA decreased as the reaction proceeded. The HMWA hydrolysate and purified GlcAcvGlc were analyzed by HPIC and TLC, respectively

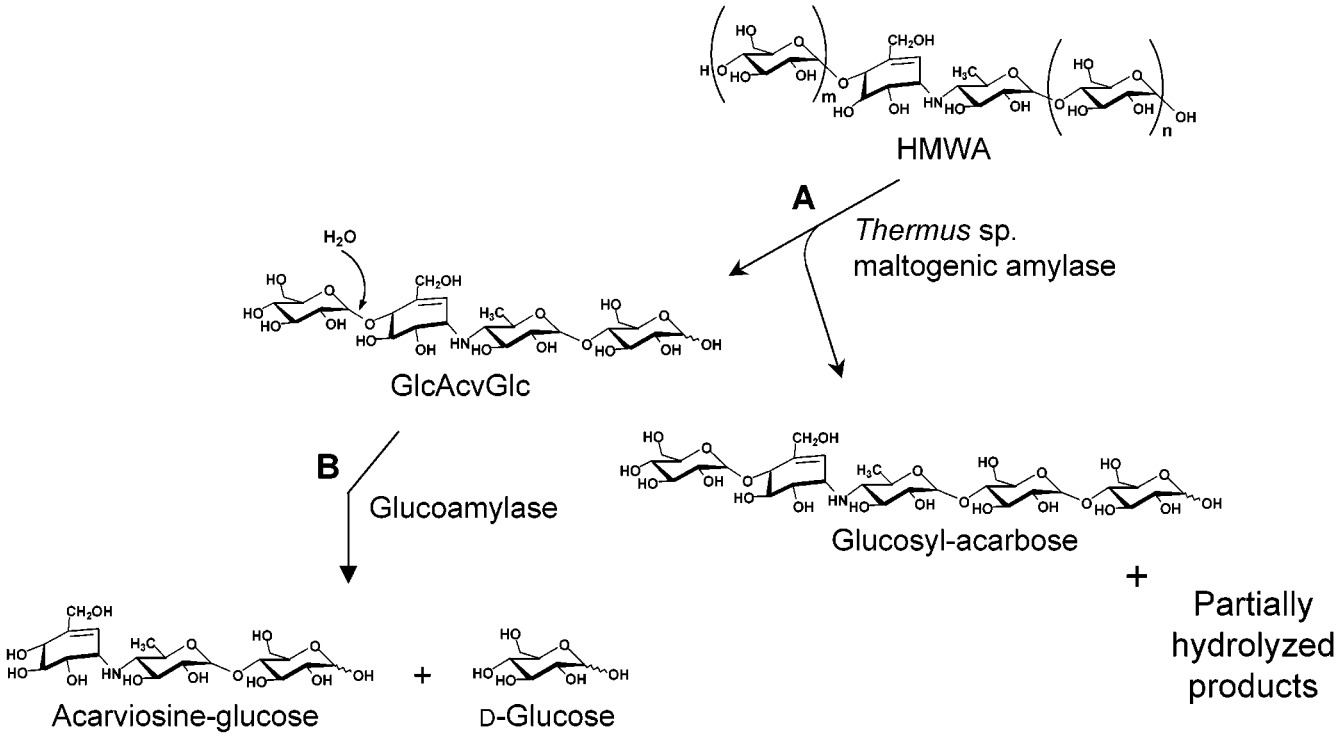

FIGURE 2: Scheme for the production of GlcAcvGlc. HMWA was produced in the culture broth by *Actinoplanes* sp. KCTC9162 using starch as a carbon source. Hydrolysis of HMWA by ThMA produced GlcAcvGlc and other analogues (A). GlcAcvGlc was degraded to D-glucose and acarviosine-glucose by glucoamylase (B).

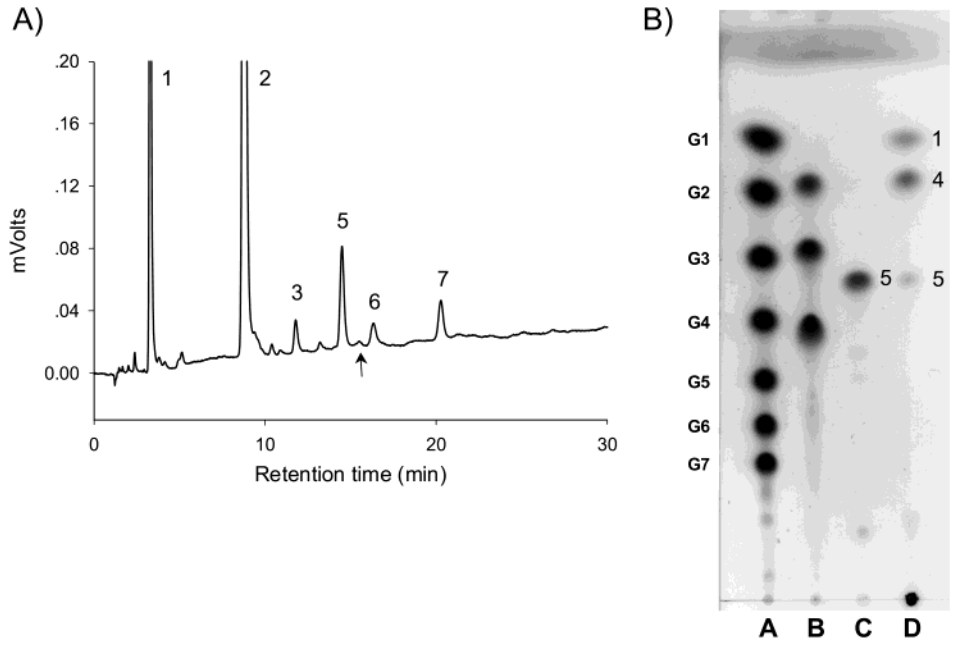

FIGURE 3: HPIC and TLC analyses of GlcAcvGlc. A, HPIC of HMWA hydrolysate by ThMA; and B, TLC of GlcAcvGlc digested with glucoamylase from *Aspergillus niger*. 100 μL of GlcAcvGlc (0.5%, w/v) was incubated with 0.3 U of glucoamylase for 12 h at 50 °C. Lane A was spotted with maltodextrin (glucose, G1, to maltoheptaose, G7); lane B, standards of acarviosine-glucose, acarbose, and isoacarbose (top to bottom); lane C, untreated GlcAcvGlc; and lane D, GlcAcvGlc digested with glucoamylase. Peak and spot 1 represent glucose; peak 2, maltose; peak 3, panose; spot 4, acarviosine-glucose; peak and spot 5, GlcAcvGlc; peak 6, 6^2-*O*-α-maltosyl-maltose; and peak 7, glucosyl-acarbose. The arrow indicates the point at which acarbose is eluted.

(Figure 3). Besides GlcAcvGlc (peak 5), small molecules such as glucose, maltose, and glucosyl-acarbose were also produced (peaks 1, 2, and 7, respectively, in Figure 3A). A small amount of branched oligosaccharides such as panose and 6^2-*O*-α-maltosyl-maltose were produced simultaneously by the transglycosylation reaction of ThMA (Figure 3, peaks 3 and 6; *17*). GlcAcvGlc was further analyzed by TLC (Figure 3B). Although GlcAcvGlc has the same molecular weight as acarbose, the chromatographic mobility of GlcAcvGlc was slower than that of acarbose in TLC (Figure 3B, lane C). Similarly, it migrated slightly faster than acarbose in HPIC (Figure 3A, peak 5). When GlcAcvGlc was degraded by glucoamylase, glucose and acarviosine-glucose were observed.

Table 1: ^{13}C NMR Signals (unit: ppm) of GlcAcvGlc

carbon atoms[b]		GlcAcvGlc	acarviosine-glucose	D-glucose	differences
ring I	1	92.7	92.7		0.0
	2	74.1	74.1		0.0
	3	75.4	75.4		0.0
	4	77.8	77.9		0.1
	5	71.5	71.3		0.2
	6	61.5	61.5		0.0
ring II	1	100.5	100.6		0.1
	2	70.8	70.8		0.0
	3	73.3	73.4		0.1
	4	64.9	65.6		0.7
	5	70.0	70.0		0.0
	6	18.2	18.2		0.0
ring III	1	55.9	56.9		1.0
	2	72.1	72.1		0.0
	3	73.8	73.7		0.1
	4	76.6	72.0		4.6
	5	126.1	124.2		1.9
	6	137.9	140.1		2.2
	7	62.8	62.4		0.4
ring IV	1	98.4		92.9	5.5
	2	72.2		72.2	0.0
	3	73.5		73.5	0.0
	4	70.2		70.4	0.2
	5	77.0		76.5	0.5
	6	61.3		61.4	0.1

[a] ^{13}C signals of acarviosine-glucose and D-glucose were obtained from comparison with those of standard compounds, acarviosine-glucose and D-glucose. [b] Numbering of the carbon of GlcAcvGlc are as follows:

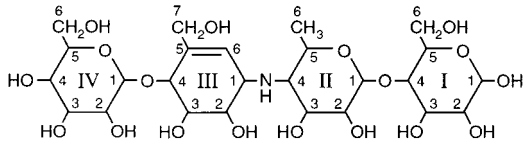

Structure Determination of GlcAcvGlc. To determine the structure of GlcAcvGlc, we obtained its ^{13}C NMR spectrum and listed the signals in Table 1. The chemical shift, 72.0 ppm, for C-4 of the cyclohexenyl ring (Ring III) of acarviosine-glucose moved upfield in case of GlcAcvGlc with the chemical shift of 76.6 ppm. Smaller chemical shifts were observed for the other carbon atoms. The large chemical shift of the carbon, C-4 of cyclohexenyl ring of GlcAcvGlc indicates the presence of a glycosidic linkage at this position. Thus, the structure of GlcAcvGlc was determined as α-D-glucopyranosyl-(1→4)-[4,5,6-trihydroxy-3-(hydroxy-methyl)-2-cyclohexen-1-yl]-[4-amino-4-deoxy-α-D-glucopyranosyl]-(1→4)-D-glucose.

The molecular weight of purified GlcAcvGlc was analyzed using a MALDI-TOF mass spectrometer (data not shown). Three peaks appeared in a spectrum at masses (*m*/*z*) of 646.6, 668.5, and 684.7. Each peak corresponds to GlcAcvGlc (M) combined with a proton ($[M + H]^+$), a sodium ion ($[M + Na]^+$), and a potassium ion ($[M + K]^+$), respectively. From the result, the molecular weight of GlcAcvGlc was determined as 645.6, which was in accordance with that of acarbose, 645.63.

To confirm the structure of GlcAcvGlc, it was incubated with glucoamylase from *Aspergillus niger* and analyzed the reaction mixture by TLC (Figure 3B, lane D). Most GlcAcvGlc was hydrolyzed to D-glucose and acarviosine-glucose by glucoamylase. This result indicated that the D-glucose molecule at the nonreducing end of GlcAcvGlc was released by the action of glucoamylase and the remnant was acarviosine-glucose. Thus, it was postulated that GlcAcvGlc had a D-glucose unit linked to the nonreducing end of acarviosine-glucose, which correlated with the NMR data.

These results indicated that the structure of GlcAcvGlc differed from that of acarbose in the position of D-glucose (Figure 1, panels A and C). That is, in acarbose, a D-glucose unit is linked to the reducing end of acarviosine-glucose, while the D-glucose of GlcAcvGlc is linked to the nonreducing end of acarviosine-glucose. Consequently, the linkage in the middle of the pseudotetrasaccharide molecule is modified with an amino group, which is not likely to be cleaved by an enzyme. Therefore, GlcAcvGlc will likely to be useful for inhibiting amylolytic enzymes that hydrolyze starch to maltose units by cleavage of the C-4 linkage.

Time-Dependent Inhibition of MGase by Acarbose and GlcAcvGlc. To investigate the inhibitory effect of acarbose and GlcAcvGlc on maltose-producing enzymes, we assayed MGase activity with the inhibitors. MGase showed time-dependent inhibition in the presence of acarbose or GlcAcvGlc (Figure 4, panels A and B). The reaction rate of the enzyme decreased gradually as the reaction proceeded and finally reached a steady-state velocity (v_s). While the initial velocity (v_0) of the reaction was independent of the concentration of both inhibitors, v_s was reduced. As shown in Figure 4, the progress curve was linear in the absence of the inhibitors, which indicated that there was no effect caused by substrate depletion. The progress curves obtained using various concentrations of the inhibitors were fitted to eq 1 to determine v_0, v_s, and k_{obs}. The plots for k_{obs} versus [I] are shown in panels C and D in Figure 4. Each plot shows linear dependence on the concentration of the inhibitors, which is one of typical properties of mechanism A involving single step of inhibition (*23*). In mechanism A, the plot for k_{obs} versus [I] should be straight line with the following equations (*16*):

$$k_{obs} = k_4 + \frac{k_3[I]}{1 + [S]/K_m} \quad (2)$$

$$K_i = \frac{k_4}{k_3} \quad (3)$$

where [I] and [S] are the concentration of inhibitor and substrate, respectively, k_3 and k_4 are the association and dissociation rate constants of E·I complex, respectively, K_i is a dissociation constant of E·I complex, and K_m is the Michaelis constant. The K_m value of the substrate, PNPG2, was 7.0 mM for MGase. The results of initial velocity and plots of k_{obs} versus [I] indicated that the inhibition of MGase by acarbose or GlcAcvGlc followed mechanism A. The kinetic parameters, k_3 and k_4, were estimated by fitting the plots of k_{obs} versus [I] to the eq 2, and then the K_i value was calculated using the eq 3 (Table 2). The K_i value of GlcAcvGlc, 0.44 nM, was far smaller than the 0.25 μM of acarbose, showing that the inhibitory activity of GlcAcvGlc toward MGase was about 560 times more potent than that of acarbose. The association rate constant (k_3) of GlcAcvGlc, 147 $\mu M^{-1}min^{-1}$, was much larger than that of acarbose, 0.0647 $\mu M^{-1}min^{-1}$. The result indicated that the rate of

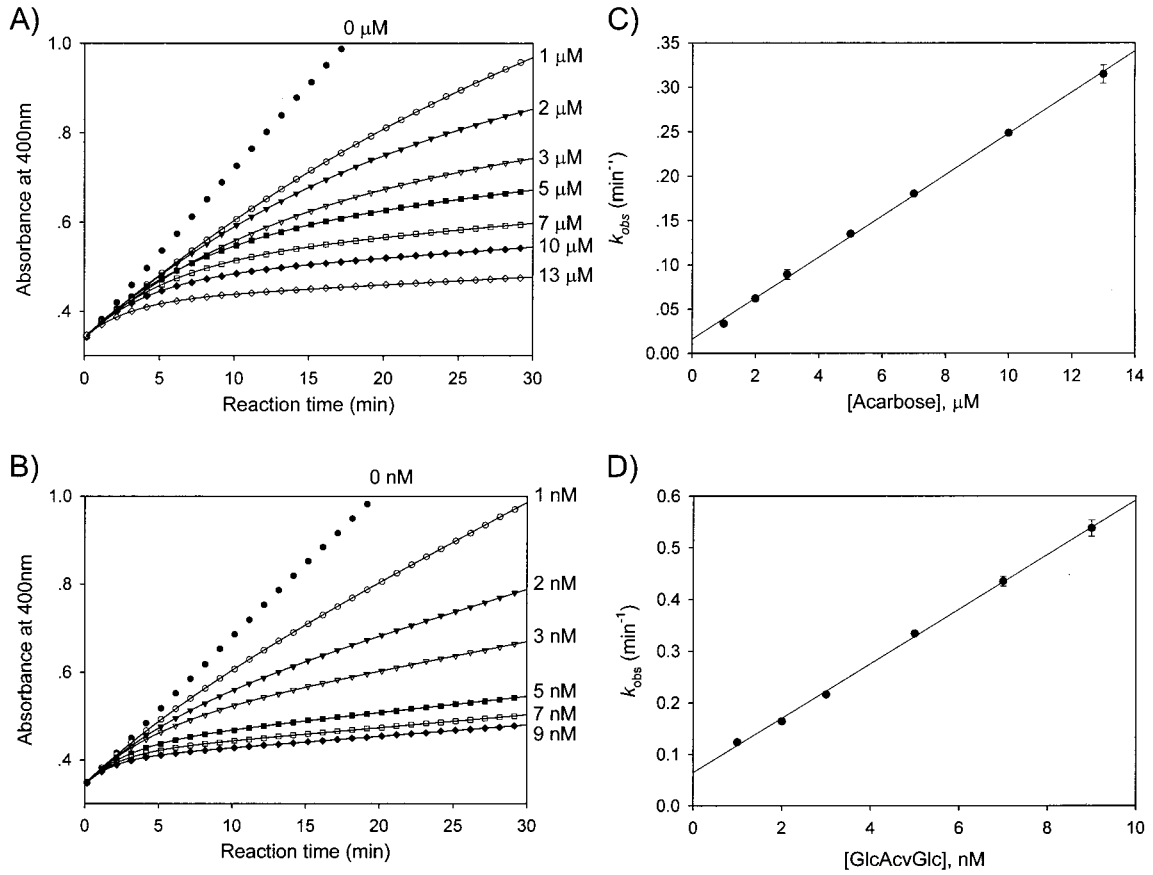

FIGURE 4: Time-dependent inhibition of MGase in the presence of acarbose and GlcAcvGlc. MGase was added to the reaction mixture containing a substrate, PNPG2, and various concentrations of inhibitors. The final concentration of the enzyme was 0.5 nM. Progress curves for acarbose (panel A) and for GlcAcvGlc (panel B) were obtained continuously, but only 30 data points are shown for clarity. The time-dependent loss in activity was fit to eq 1 (solid lines). The pseudo-first-order rate constants (k_{obs}) derived from the fit are plotted against the concentrations of inhibitors (panel C for acarbose and D for GlcAcvGlc). The straight lines represent the best fits of the data to eq 2, and the kinetic parameters (k_3, k_4) are derived from the fits. Error bars are standard deviations from duplicate data sets.

Table 2: Kinetic Parameters for the Time-Dependent Inhibition of Amylases by Acarbose and GlcAcvGlc

		kinetic parameters[a] (mechanism A)			kinetic parameters[a] (mechanism B)					
enzyme	inhibitors	k_3 (μM^{-1} min^{-1})	k_4 (min^{-1})	K_I (nM)	k_5 (min^{-1})	k_6 (min^{-1})	k_5/k_6	K_i (μM)	K_i* (nM)	potency[b]
MGase	acarbose	0.0647 ± 0.0008	0.0160 ± 0.0014	247 ± 18						1
	GlcAcvGlc	147 ± 7	0.0643 ± 0.0063	0.439 ± 0.062						563
ThMA	acarbose				0.374 ± 0.010	0.0173 ± 0.0063	21.6	8.18 ± 0.60	362 ± 135	1
	GlcAcvGlc				3.61 ± 0.32	0.0333 ± 0.0074	108.4	0.0272 ± 0.0033	0.249 ± 0.067	1450
CDase I-5	acarbose				0.593 ± 0.038	0.0200 ± 0.0057	29.7	25.2 ± 3.5	822 ± 266	1
	GlcAcvGlc				3.30 ± 0.28	0.0688 ± 0.0100	48.0	0.0369 ± 0.0081	0.754 ± 0.208	1090

[a] These values were derived from k_{obs} vs [I] plots by fitting the data to eq 2 − eq 5. [b] Potency was calculated by dividing the K_i (or K_i*) of acarbose with the K_i (or K_i*) of GlcAcvGlc.

MGase−GlcAcvGlc complex formation was faster and the binding affinity of GlcAcvGlc to MGase was better than those of acarbose.

Time-Dependent Inhibition of ThMA and CDase I-5 by Acarbose and GlcAcvGlc. The progress curves of ThMA and CDase I-5 were also hyperbolic representing slow-binding inhibition (Figure 5, panels A and B; Figure 6, panels A and B). In contrast to MGase, the initial velocity (v_0) and the steady-state velocity (v_s) decreased as the concentration of the inhibitors increased in assays with ThMA and CDase I-5. In general, one of the different properties between mechanism A and B is the constancy of initial velocity in the presence of slow-binding inhibitor (*24*). That is, v_0 does not vary with [I] in mechanism A but decreases in mechanism B. Also, the plot of k_{obs} versus [I] is not linear but hyperbolic in mechanism B, and the relationship can be described as the following equations:

$$k_{obs} = k_6 + \frac{k_5[I]/K_i}{1 + [S]/K_m + [I]/K_i} \quad (4)$$

where k_5 and k_6 are the forward and reverse isomerization

$$K_i^* = K_i \frac{k_6}{k_5 + k_6} \quad (5)$$

rate constants, respectively, and K_i* is the overall inhibition constant. The K_m values of PNPG2 were 0.20 and 0.18 mM

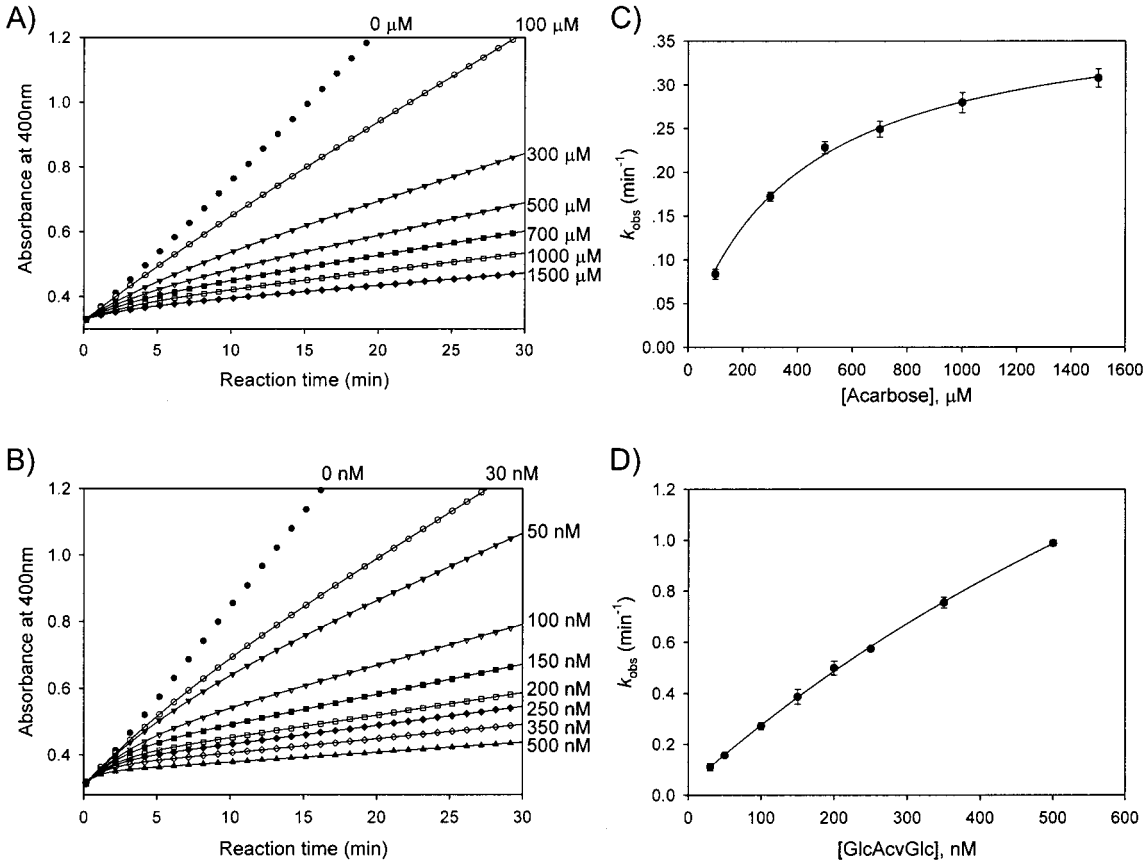

FIGURE 5: Time-dependent inhibition of ThMA in the presence of acarbose and GlcAcvGlc. Each curve was obtained as described in the legend to Figure 4. The final concentration of the enzyme was 3.4 nM. In panels C and D, the curves represent the best fits of the data to eq 4, and the kinetic parameters (K_i, k_5, k_6) are derived from the fits. Error bars are standard deviations from duplicate data sets.

for ThMA and CDase I-5, respectively. The transition rate constants (k_{obs}) of ThMA and CDase I-5 showed a hyperbolic dependence on the concentration of the inhibitor (Figure 5, panels C and D; Figure 6, panels C and D), so the inhibitions of ThMA and CDase I-5 by both inhibitors followed mechanism B. The kinetic parameters, k_5, k_6, K_i, and K_i*, were derived from the plots by fitting the results to eqs 4 and 5 and summarized in Table 2. Both acarbose and GlcAcvGlc acted as slow-binding inhibitors for ThMA and CDase I-5. The overall inhibition constants (K_i*) of GlcAcvGlc were far smaller than those of acarbose. K_i* of GlcAcvGlc for ThMA and CDase I-5 was 0.25 and 0.75 nM, respectively, while that of acarbose was 0.36 and 0.82 μM, respectively. In other words, inhibitor potencies of GlcAcvGlc for ThMA and CDase I-5 were 3 orders of magnitude superior to those of acarbose. Also, forward rate constants (k_5) for the isomerization of the enzyme−GlcAcvGlc intermediate to a more stable complex is about 10 times larger than those for enzyme−acarbose complex. The result reveals that GlcAcvGlc is a more suitable inhibitor converting the enzyme−inhibitor intermediate into the more stable form. Since the faster forward isomerization rate of the enzyme−inhibitor complex causes the shorter duration time of the complex, the steady-state concentration of E·I is decreased, and the inhibition seems to follow mechanism A (*16*). To determine the mode of time-dependent inhibition, a plot of $1/(k_{obs} - k_6)$ versus 1/[I] may be useful (*25*). The *y*-intercept of the linear plot is positive in mechanism B represented by $1/k_5$, while it is zero in mechanism A (Figure 7). The plots for GlcAcvGlc and acarbose against ThMA gave the intercepts of 0.31 and 2.45, respectively. The positive values of the intercept confirmed that both enzymes were inhibited in the mode of mechanism B.

Inhibition of Other Amylolytic Enzymes by GlcAcvGlc. Table 3 shows the IC_{50} values of several amylolytic enzymes in the presence of acarbose or GlcAcvGlc. Although both maltase and sucrase from rat intestine were inhibited more efficiently by acarbose than by GlcAcvGlc, α-amylase from porcine pancreas (PPA) was more sensitive to GlcAcvGlc than acarbose. GlcAcvGlc was most effective for ThMA as expected. IC_{50} of GlcAcvGlc for ThMA, 68 nM, which was significantly less than the IC_{50} (340 nM) of acarbose, indicatied that GlcAcvGlc was a much better inhibitor of ThMA. Neither GlcAcvGlc nor acarbose was an inhibitor for sweet potato β-amylase.

Effect of GlcAcvGlc on the Quaternary Structure of ThMA. ThMA is present in equilibrium between monomer and dimer in solution (*22*). In the ThMA dimer, the N-terminus of one unit covered the top part of the active site of the other unit, which makes the enzyme active site narrow and deep (*22*). The dimeric form of ThMA increased significantly from 46.8% to 81.0% by adding 30 μM of GlcAcvGlc to the enzyme solution (Table 4). This indicates that the monomer/dimer equilibrium was shifted to dimeric form in the presence of the inhibitor. This result is supported by the X-ray crystallographic analysis of ThMA crystals complexed with GlcAcvGlc (Figure 8). Residues from both the $(\beta/\alpha)_8$ barrel of one subunit and the N-terminal domain of the other subunit are involved in the binding of the inhibitor, inducing the dimeric state of ThMA. GlcAcvGlc binds in the catalytic

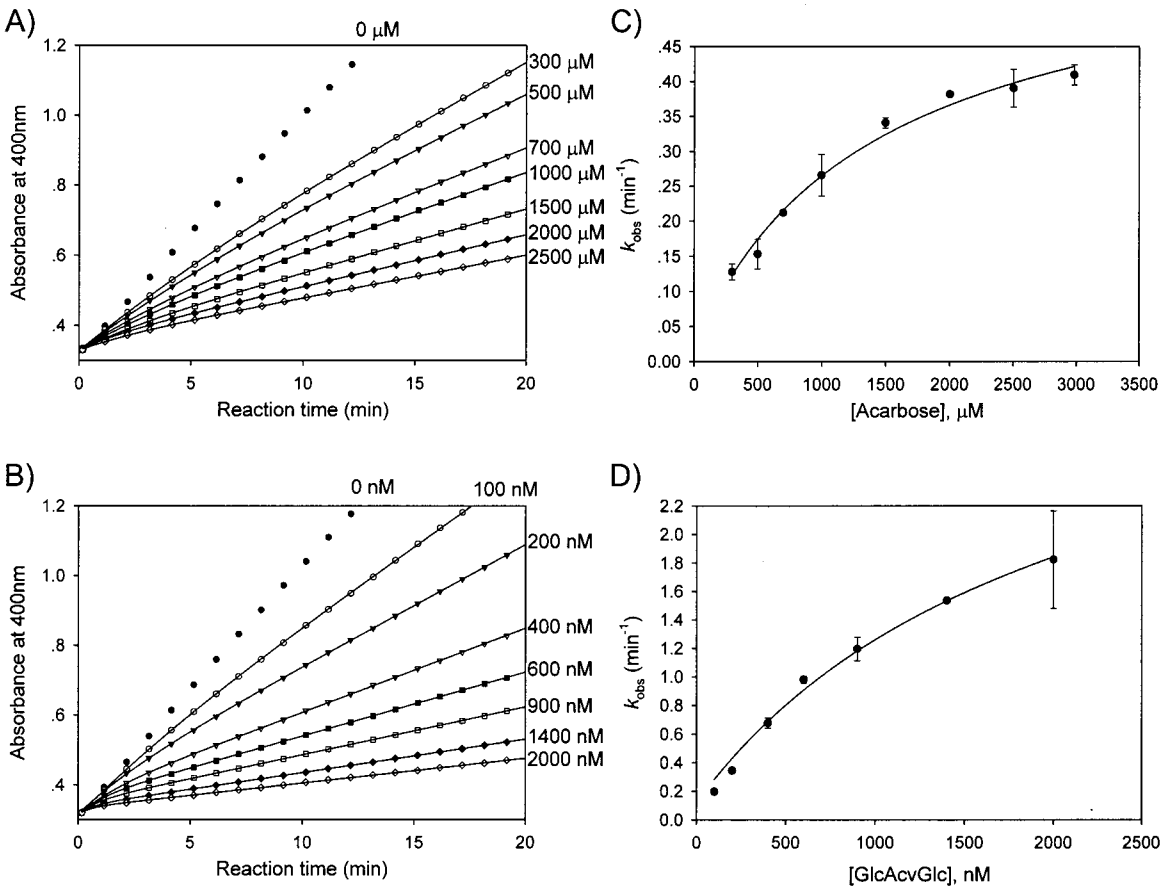

FIGURE 6: Time-dependent inhibition of CDase I-5 in the presence of acarbose and GlcAcvGlc. Each curve was obtained as described in the legend to Figure 4. The final concentration of the enzyme was 8.1 nM. In panels C and D, the curves represent the best fits of the data to eq 4, and the kinetic parameters (K_i, k_5, k_6) are derived from the fits. Error bars are standard deviations from duplicate data sets.

residues (Asp328, Glu357, and Asp424) of one subunit by hydrogen bonds. In additions, residues (Tyr45, Arg83, and Asp110) in the N-terminus of the other subunit also interact with the deoxyglucose unit and reducing end of GlcAcvGlc. Due to the additional hydrogen bonds, the ThMA−GlcAcvGlc intermediate is supposed to form a more stable complex. From these results, GlcAcvGlc in the reaction mixture is likely to favorably induce the dimerization of ThMA, thereby stabilizing the enzyme−inhibitor complex and being responsible for the two-step inhibition via mechanism B of slow-binding inhibition.

DISCUSSION

In the present study, we described the production of GlcAcvGlc and its inhibition properties for maltose-producing enzymes including MGase, ThMA, CDase I-5, and some other amylolytic enzymes. Junge et al. (*26*) prepared acarviosine−glucose, acarviosine, and some byproducts from acarbose by acid hydrolysis, but not GlcAcvGlc by the procedure. Both GlcAcvGlc and acarbose showed time-dependent inhibitions against MGase, ThMA, and CDase I-5. The inhibition of ThMA and CDase I-5 by acarbose or GlcAcvGlc followed mechanism B, while that of MGase followed mechanism A in Scheme 1. To explain the difference in inhibition mechanism between MGase and ThMA (or CDase I-5), the oligomeric state of the enzymes should be taken into consideration as a major factor among several possibilities. Recently, ThMA was reported to be in equilibrium between monomer and dimer in solution, and its substrate specificity was dependent on the oligomeric state of ThMA (*22*, *27*). Moreover, analytical ultracentrifugation study and X-ray crystallography of ThMA-GlcAcvGlc complex indicated that GlcAcvGlc promoted the shift toward dimer from monomer of ThMA in solution (Table 4 and Figure 8). A similar phenomenon of substrate-induced oligomerization was observed in NADPH:FMN oxidoreductase from *Vibrio harveyi* (*28*) in which binding of flavin mononucleotide to the apoenzyme promoted dimerization of the enzyme with a decrease of dissociation constant from 3.3 to 1.8 μM. In the case of the RNA polymerase from *Sulfolobus shibatae*, the 48 kDa monomer forms a stable salt-resistant dimer in solution (*29*) and further dimerization of the dimeric enzyme to a tetramer is induced by the binding of two tRNA molecules. Therefore, the slow-binding mechanism B seems to be associated with the change in the quaternary structure of ThMA. Dimerization of ThMA induced by the formation of the ThMA−GlcAcvGlc complex causes the secondary conformational change of the enzyme−inhibitor complex. CDase I-5 forms a dodecamer (*30*); therefore, it may behavior similarly to ThMA. In contrast, MGase exists exclusively as a monomer (*31*) and is inhibited by GlcAcvGlc following mechanism A.

GlcAcvGlc showed strong inhibitory effect especially on the maltose-producing amylases such as MGase, ThMA, and CDase I-5 (Table 2). For the three enzymes tested, K_i and K_i^* of GlcAcvGlc were in the nanomolar range, while those

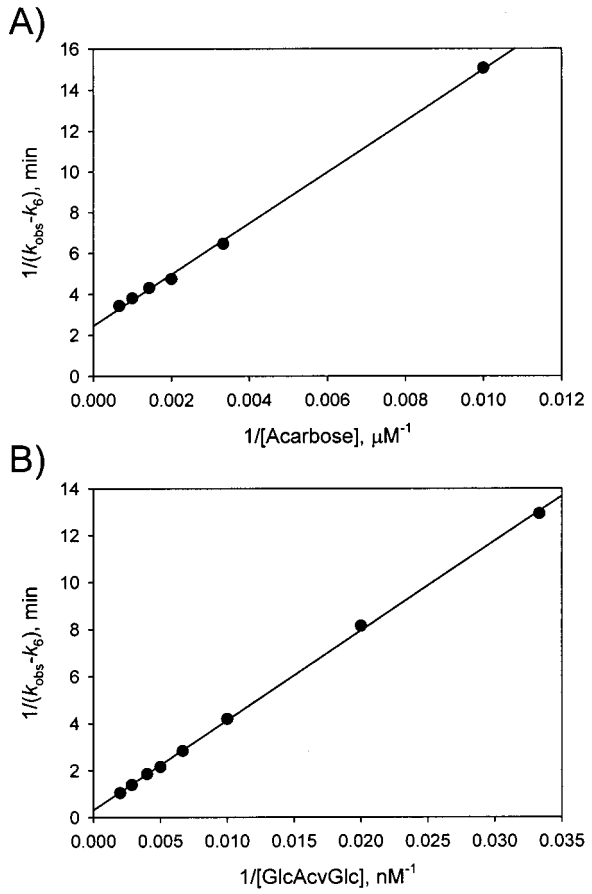

FIGURE 7: $1/(k_{obs} - k_6)$ vs 1/[inhibitor] for the interaction of inhibitors with ThMA. (A) acarbose; and (B) GlcAcvGlc. Values for k_{obs} and k_6 were obtained as described in the legend to Figure 5. The lines cross the positive *y*-axis at the points equal to $1/k_5$.

Table 3: Inhibitory Activities of Acarbose and GlcAcvGlc against Various Amylolytic Enzymes

	IC_{50}[a] (μM)		
enzymes[b]	acarbose	GlcAcvGlc	potency[d]
maltase	0.24 ± 0.01	4.1 ± 0.2	0.058
sucrase	0.96 ± 0.01	8.1 ± 0.2	0.12
α-amylase	2.7 ± 0.3	1.2 ± 0.2	2.2
β-amylase	N[c]	N[c]	–
ThMA	340 ± 30	0.068 ± 0.01	5040

[a] The IC_{50} value represents the concentration of an inhibitor causing 50% decrease of the enzyme activity. The values are the means ± S.D. of three separate experiments. [b] Maltase and sucrase are from rat intestine; α-amylase, porcine pancreas; β-amylase, sweet potato; and ThMA, a maltogenic amylase from *Thermus* sp. [c] No inhibition was observed at 1 mM of the inhibitors. [d] Potency was calculated by dividing the IC_{50} of acarbose with the IC_{50} of GlcAcvGlc.

of acarbose were in the micromolar range; that is, the inhibition potency of GlcAcvGlc was about 3 orders of magnitude better than that of acarbose. Since ThMA readily hydrolyzes maltotetraose to two molecules of maltose rather than glucose and maltotriose (*17*), binding of maltotetraose at the −2 to +2 subsite of ThMA is supposed to be thermodynamically most favorable. The binding pattern of GlcAcvGlc seems to be similar to that of maltotetraose, which is located at the −2 to +2 subsite so that the acarviosine unit is positioned at the −1 to +1 subsite of ThMA. The X-ray crystallographic structure of the ThMA−

Table 4: Monomer/Dimer Equilibrium of ThMA in the Presence of GlcAcvGlc[a]

GlcAcvGlc (μM)	$K_{1,2}$[b] (M)	monomer (%)[c]	dimer (%)[c]
0.0	$(7.04 \pm 0.44) \times 10^{-7}$	53.2	46.8
0.075	$(2.14 \pm 0.19) \times 10^{-7}$	36.2	63.8
1.5	$(1.46 \pm 0.07) \times 10^{-7}$	31.4	68.6
30.0	$(4.23 \pm 0.98) \times 10^{-8}$	19.0	81.0

[a] The ratios of monomer and dimer were determined by fitting the analytical ultracentrifugation data obtained at 4 °C (*21*). The concentration of ThMA was 0.117 mg/mL. [b] The dissociation constant between dimer and monomer of ThMA in solution (*21*). The values are the means ± S.D. of three separate experiments. [c] Molar ratio.

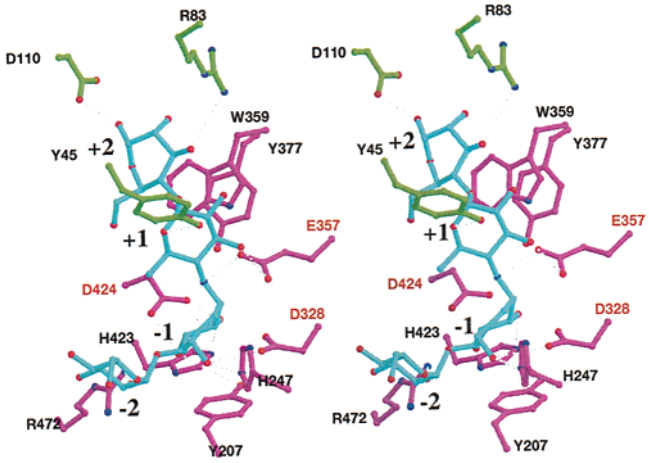

FIGURE 8: Binding of GlcAcvGlc at the active site of ThMA. The crystals of ThMA complexed with GlcAcvGlc were obtained by soaking the inhibitor into the native crystal (*22*). Residues from both the $(\beta/\alpha)_8$ barrel (from one subunit) and the N-terminal domain (from the other subunit) are involved in the binding of the inhibitor and are shown in magenta and green, respectively. The three catalytic residues are labeled in red. Hydrogen bonds are indicated as dotted lines. The figure was produced using the program MOLSCRIPT (*36*). Diffraction data to 2.55 Å were obtained from a flash-cooled crystal using the synchrotron X-ray beamline BL6B at Photon Factory (Tsukuba, Japan). Experimental detail and full description of the structure was described in Materials and Methods.

GlcAcvGlc complex (Figure 8) indicates that the linkage to be cleaved lies between unsaturated cyclitol and 4-amino-4,6-dideoxy glucose close to the catalytic residues of Asp328, Glu357, and Asp424. CDase I-5 and MGase also produce maltose mainly from linear maltooligosaccharides (*32*, *33*), and the subsite location of the inhibitor is likely to be identical to that of ThMA. Besides acarbose inhibited ThMA with less inhibitory effect than GlcAcvGlc, it could be hydrolyzed into acarviosine-glucose and glucose by ThMA. Therefore, the acarviosine moiety of acarbose is supposed to locate at either the −1 to +1 (when inhibiting) or the −2 to −1 (when being hydrolyzed) subsite of ThMA (*21*). From this reason, GlcAcvGlc showed a better inhibition than acarbose for maltose-producing enzymes. GlcAcvGlc inhibited PPA more effectively than acarbose (Table 3). This result is reasonable considering the catalytic properties of amylases. When maltotetraose specifically labeled in the reducing glucose unit was treated with PPA, 70% of maltotetraose was hydrolyzed to maltose and labeled maltose, while the first glycosidic linkage from nonreducing end was hardly cleaved (*34*). That is, the most favorable binding

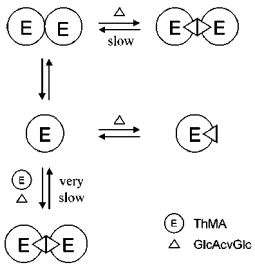

FIGURE 9: Schematic model for GlcAcvGlc binding to ThMA monomer or dimer. Binding of the inhibitor does not cause further conformational change of the dimeric enzyme, but the inhibitor binds to the dimeric enzyme with higher affinity than to the monomeric enzyme.

position of maltotetraose is at the −2 to +2 subsite of PPA, which indicates that GlcAcvGlc can be a more potent inhibitor than acarbose. In contrast, acarbose is a better inhibitor for maltase and sucrase. This can be explained by that acarbose binds glucose-producing enzyme at the −1 to +3 subsite in which the acarviosine unit of acarbose is located at the −1 to +1 subsite of the enzyme. GlcAcvGlc was a poor inhibitor for β-amylase from sweet potato (Table 3). This is a somewhat unexpected result because β-amylase produces maltose from starch, implying that β-amylase might be a target enzyme of GlcAcvGlc. This result provides an indirect information that the action mechanism or substrate binding mode of β-amylase may be different from the mechanisms for other amylolytic enzymes. Actually, the primary structure of β-amylase is quite different among them (*35*).

From the above results, we suggest that the slow-binding phenomenon observed for the inhibition of maltose-producing α-amylase by GlcAcvGlc is caused by a slow dissociation step of the inhibitor−dimeric enzyme complex, as illustrated in Figure 9. GlcAcvGlc binds to the active site cleft of the dimeric form of the enzyme with high affinity. Moreover, the inhibitor induces the shift of the monomer−dimer equilibrium to the dimeric form of the enzyme, which elicits further increase in the concentration of the inhibitor-dimeric enzyme complex. The dimer−inhibitor complex with higher affinity might result in slow-binding inhibition of mechanism B.

SUPPORTING INFORMATION AVAILABLE

MALDI-TOF mass spectrum of purified GlcAcvGlc. This material is available free of charge via the Internet at http://pubs.acs.org.

REFERENCES

1. Schmidt, D. D., Frommer, W., Junge, B., Müller, L., Wingender, W., and Truscheit, E. (1981) in *First International Symposium on Acarbose* (Creutzfeldt, E. W., Ed.) pp 5−15, Excerpta Medica, Amsterdam.
2. Aleshin, A. E., Firsov, L. M., and Honzatko, R. B. (1994) *J. Biol. Chem. 269*, 15631−15639.
3. Svensson, B., and Sierks, M. R. (1992) *Carbohydr. Res. 227*, 29−44.
4. Brzozowski, A. M., and Davies, G. J. (1997) *Biochemistry 36*, 10837−10845.
5. Alkazaz, M., Desseaux, V., Marchis-Mouren, G., Payan, F., Forest, E., and Santimone, M. (1996) *Eur. J. Biochem. 241*, 787−796.
6. Strokopytov, B., Penninga, D., Rozeboom, H. J., Kalk, K. H., Dijkhuizen, L., and Dijkstra, B. W. (1995) *Biochemistry 34*, 2234−2240.
7. Kim, M. J., Lee, S. B., Lee, H. S., Lee, S. Y., Baek, J. S., Kim, D., Moon, T. W., Robyt, J. F., and Park, K. H. (1999) *Arch. Biochem. Biophys. 371*, 277−283.
8. Fierobe, H. P., Clarke, A. J., Tull, D., and Svensson, B. (1998) *Biochemistry 37*, 3753−3759.
9. Park, K. H., Kim, M. J., Lee, H. S., Han, N. S., Kim, D., and Robyt, J. F. (1998) *Carbohydr. Res. 313*, 235−246.
10. Bischoff, H. (1995) *Clin. Invest. Med. 18*, 303−311.
11. Schöffling, K., Hillebrand, I., and Berchtold, P. (1980) *Front. Hormone Res. 7*, 248−257.
12. Hanozet, G., Pircher, H.-P., Vanni, P., Oesch, B., and Semenza, G. (1981) *J. Biol. Chem. 256*, 3703−3711.
13. Lohse, A., Hardlei, T., Jensen, A., Plesner, I. W., and Bols, M. (2000) *Biochem. J. 349*, 211−215.
14. Ando, O., Nakajima, M., Kifune, M., Fang, H., and Tanzawa, K. (1995) *Biochim. Biophys. Acta 1244*, 295−302.
15. Binderup, K., Libessart, N., and Preiss, J. (2000) *Arch. Biochem. Biophys. 374*, 73−78.
16. Morrison, J. F., and Walsh, C. T. (1988) *Adv. Enzymol. Relat. Areas Mol. Biol. 61*, 201−301.
17. Kim, T. J., Kim, M. J., Kim, B. C., Kim, J. C., Cheong, T. K., Kim, J. W., and Park, K. H. (1999) *Appl. Environ. Microbiol. 65*, 1644−1651.
18. Kim, T. J., Shin, J. H., Oh, J. H., Kim, M. J., Lee, S. B., Ryu, S., Kwon, K., Kim, J. W., Choi, E. H., Robyt, J. F., and Park, K. H. (1998) *Arch. Biochem. Biophys. 353*, 221−227.
19. Segel, I. H. (1975) in *Enzyme Kinetics*, pp 46−49, John Wiley & Sons, New York.
20. Fox, J. D., and Robyt, J. F. (1991) *Anal. Biochem. 195*, 93−96.
21. Kim, T. J., Park, C. S., Cho, H. Y., Cha, S. S., Kim, J. S., Lee, S. B., Moon, T. W., Kim, J. W., Oh, B. H., and Park, K. H. (2000) *Biochemistry 39*, 6773−6780.
22. Kim, J. S., Cha, S. S., Kim, H. J., Kim, T. J., Ha, N. C., Oh, S. T., Cho, H. S., Cho, M. J., Kim, M. J., Lee, H. S., Kim, J. W., Choi, K. Y., Park, K. H., and Oh, B. H. (1999) *J. Biol. Chem. 274*, 26279−26286.
23. Duggleby, R. G., Attwood, P. V., Wallace, J. C., and Keech, D. B. (1982) *Biochemistry 21*, 3364−3370.
24. Copeland, R. A. (1996) in *Enzymes*, pp 237−261, Wiley-VCH, New York.
25. Dahlen, J. R., Foster, D. C., and Kisiel, W. (1999) *Biochim. Biophys. Acta 1451*, 233−241.
26. Junge, B., Boshagen, H., Stoltefuss, J., and Müller, L. (1980) in *Enzyme Inhibitors* (Brodbeck, U., Ed.) pp 123−137, Verlag Chemie, Weinheim, Germany.
27. Park, K. H., Kim, T. J., Cheong, T. K., Kim, J. W., Oh, B. H., and Svensson, B. (2000) *Biochim. Biophys. Acta 1478*, 165−185.
28. Liu, M., Lei, B., Ding, Q., Lee, J. C., and Tu, S. C. (1997) *Arch. Biochem. Biophys. 337*, 89−95.
29. Li, F., Wang, J., and Steitz, T. A. (2000) *J. Mol. Biol. 304*, 483−492.
30. Park, K. H. (2001) *J. Appl. Glycosci. 48*, 293−299.
31. Dauter, Z., Duater, M., Brzozowski, A. M., Christensen, S., Borchert, T. V., Beier, L., Wilson, K. S., and Davies, G. J. (1999) *Biochemistry 38*, 8385−8392.
32. Kim, M. J., Park, W. S., Lee, H. S., Kim, T. J., Shin, J. H., Yoo, S. H., Cheong, T. K., Ryu, S., Kim, J. C., Kim, J. W., Moon, T. H., Robyt, J. F., and Park, K. H. (1999) *Arch. Biochem. Biophys. 373*, 110−115.
33. Outtrup, H., and Norman, B. E. (1984) *Starch/Stärke 36*, 405−411.
34. Robyt, J. F., and French, D. (1970) *J. Biol. Chem. 245*, 3917−3927.
35. Mikami, B., Hehre, E. J., Sachettini, J. C., and Morita, Y. (1995) in *Enzyme Chemistry and Molecular Biology of Amylases and Related Enzymes* (Yamamoto, T., Ed.) pp 145−153, CRC Press, Boca Raton, FL.
36. Esnouf, R. M. (1997) *J. Mol. Graph. Model. 15*, 132−134.

BI025586B